Prio-IMU: Prioritizable IMU Array for Enhancing Foot-mounted Inertial Navigation Accuracy

Chi-Shih Jao, Danmeng Wang, and Andrei M. Shkel
Department of Mechanical And Aerospace Engineering, University of California, Irvine
{chishihj,danmenw,andrei.shkel}@uci.edu

***Abstract*—This paper presents a prioritizable Inertial Measurement Unit (IMU) array, referred to as the Prio-IMU, which is a systematic approach to mitigate the problem of insufficient sensor's Full-Scale Range (FSR) and bandwidth, in the case of foot-mounted Inertial Navigation Systems (INS). The Prio-IMU integrates multiple IMUs with different sensor characteristics, aligns all the sensor measurements to a universal coordinate frame, and prioritizes the usage of each integrated sensor based on different scenarios. We developed a Prio-IMU prototype integrating two IMUs (ICM-20948 and ICM-20649) and a 3-axis accelerometer (ADXL375) and conducted a series of pedestrian navigation experiments involving walking and running. We observed that during the heel-strike phases of running activity, accelerometer and gyroscope measurements as large as 70 [gravity (g)] and 2600 [degree per second (dps)] could be picked up by the developed Prio-IMU prototype. The experimental results showed that the navigation accuracy of the Zero-velocity-UPdaTe (ZUPT)-aided INS using the proposed Prio-IMU was improved by 79% and 82% along the horizontal and vertical directions, as compared to the case of using a single IMU.**

***Index Terms*—IMU Array, ZUPT, Inertial Navigation**

I. Introduction

Development of universal pedestrian navigation systems can enable multiple critical applications, including contact tracing, asset monitoring, and firefighter localization. Systems designed for these purposes need to operate in extreme scenarios, where the Global Navigation Satellite Systems (GNSS) have degraded performance, visibility is poor due to smoke and airborne particles, and Radio-Frequency (RF) infrastructures are not accessible [1]. Foot-mounted Inertial Measurement Units (IMU) have been considered a core technology in such universal navigation systems, as inertial sensors provide self-contained measurements, and foot-mounted configurations allow for enhancing a strapdown Inertial Navigation System (INS) with a Zero-velocity UPdaTe (ZUPT) algorithm, which significantly reduces accumulated navigation errors inherent in an INS by periodically resetting velocity errors during the stance phase of a human gait cycle [2]. The ZUPT-aided INS in the case of walking has been analytically predicted and experimentally demonstrated to have a positioning error of less than 1% of traveling distances [3].

It is, however, still challenging for the ZUPT-aided INS to maintain the same level of accuracy as the case of walking while performing other common pedestrian activities, such as running, crawling, or jumping [4]. The degraded navigation performance in the case of non-walking activities is a result of several factors, including increased difficulties in robust stance phase detection, increased residual velocities during the stance phases that lead to unmodeled errors, and increased demands in inertial sensor's Full-Scale Range (FSR) and bandwidth. Many approaches have been developed to address these difficulties [5]–[7], and this paper focuses on addressing the problem of sensor's insufficient FSR and bandwidth. While performing non-walking activities, foot-mounted sensors have been shown to experience forces that generate accelerations and angular velocities exceeding 40 [gravity (g)] and 2000 [degree per second (dps)] during the toe-off and heel-strike phases in a gait cycle [8]. These forces can saturate many high-performance Commercial-Off-The-Shelf (COTS) IMUs, degrading the accuracy of the ZUPT-aided INS.

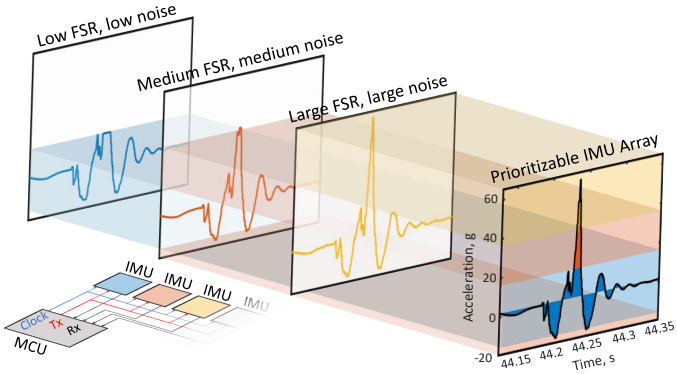

Fig. 1. Concept of the proposed Prioritizable IMU array (Prio-IMU).

Previous work on mitigating the problem of insufficient sensor FSR and bandwidth in foot-mounted IMUs attempted different approaches. In [9], the research group modified the ZUPT-aided INS algorithm by applying zero position change during heel strike phases and adjusting estimation error covariance matrices. In [10], an additional IMU mounted on the calf of a human was used to assist a foot-mounted IMU. In [8], an expensive high-performance IMU with a large sensor FSR was used to train a machine learning model that predicts saturated accelerometer measurements based on identification of saturated periods. The predictions were used to reconstruct saturated accelerometer measurements of a low-cost IMU. In [11], an IMU array integrating multiple identical IMUs was developed, and the measurement range of angular velocities could be extended by a Maximum Likelihood Estimation

This work was performed under the following financial assistance awards: 70NANB22H073 from the U.S. Department of Commerce, National Institute of Standards and Technology (NIST).

(MLE) approach. Although these approaches were shown to improve navigation accuracy, they did not universally address the problems of both insufficient FSR and bandwidth of foot-mounted inertial sensors operating in the case of pedestrians performing violent activities.

This paper reports a prioritizable IMU array (Prio-IMU), a systematic approach utilizing multiple different IMUs to mitigate the impact of insufficient sensor FSR and bandwidth on ZUPT-aided INS using foot-mounted IMUs. Fig. 1 illustrates the concept of the proposed Prio-IMU. The Prio-IMU integrates readings from multiple IMUs, each with different sensor FSRs and noise characteristics. The approach utilizes the properties that an IMU with good noise characteristics usually comes with a trade-off of low sensor FSR and bandwidth, and vice versa. In scenarios when the system experiences large accelerations and angular velocities, utilizing a sensor with great noise performance but insufficient FSR could lead to a larger navigation error, as compared to a sensor with poor noise performance but sufficiently high FSR.

II. Approach

In the proposed Prio-IMU, each IMU in the system needs to be aligned to a universal coordinate system so that all the units measure similar physical quantities of accelerations and angular velocities. This section describes a sensor model, discusses the alignment of multiple IMUs, and presents a mechanism to prioritize the usage of different IMUs.

A. Sensor model

The proposed Prio-IMU considers N calibrated IMUs mounted on different locations of a rigid body, such as a Printed Circuit Board (PCB). An IMU calibration process includes identifying errors in the sensor's scale factors, cross-axis sensitivities, and turn-on biases, and the procedure could be done with an estimation algorithm using self-measurements [12] or through external equipment, such as a shaker or a rate table [13]. The ith IMU of the Prio-IMU is characterized by eight different metrics, including accelerometer's FSR, $\mathrm{F}_{\mathrm{a}}^{i}$, bandwidth, $\mathrm{B}_{\mathrm{a}}^{i}$, Velocity Random Walk (VRW), $\sigma_{\mathrm{a,N}}^{i}$, and bias instability, $\sigma_{\mathrm{a,B}}^{i}$, and gyroscope's FSR, $\mathrm{F}_{\mathrm{g}}^{i}$, bandwidth, $\mathrm{B}_{\mathrm{g}}^{i}$, Angular Random Walk (ARW), $\sigma_{\mathrm{g,N}}^{i}$, and bias instability, $\sigma_{\mathrm{g,B}}^{i}$. The N IMUs can be chosen such that the characterization metrics satisfy the following conditions:

$$\forall i > 0 \text{ and } i < j < N, \mathrm{F}_{\mathrm{a}}^{i} \leq \mathrm{F}_{\mathrm{a}}^{j}, \mathrm{B}_{\mathrm{a}}^{i} \leq \mathrm{B}_{\mathrm{a}}^{j}, \sigma_{\mathrm{a,N}}^{i} \leq \sigma_{\mathrm{a,N}}^{j},$$

$$\sigma_{\mathrm{a,B}}^{i} \leq \sigma_{\mathrm{a,B}}^{j}, \mathrm{F}_{\mathrm{g}}^{i} \leq \mathrm{F}_{\mathrm{g}}^{j}, \mathrm{B}_{\mathrm{g}}^{i} \leq \mathrm{B}_{\mathrm{g}}^{j}, \sigma_{\mathrm{g,N}}^{i} \leq \sigma_{\mathrm{g,N}}^{j}, \sigma_{\mathrm{g,B}}^{i} \leq \sigma_{\mathrm{g,B}}^{j}.$$

The Prio-IMU produces a single measurement vector at time k, denoted as $\mathbf{u}_k$, by prioritizing the measurements collected by one of the IMUs integrated into the system. The prioritization mechanism is discussed in Section II-C. A Prio-IMU measurement vector $\mathbf{u}_k$ includes accelerometer readings, $\mathbf{a}_k$, and gyroscope readings, $\boldsymbol{\omega}_k$, along the three axes. $\mathbf{a}_k$ and $\boldsymbol{\omega}_k$ are modeled as follows:

$$\mathbf{a}_k = \bar{\mathbf{a}}_k + \bar{\mathbf{b}}_{\mathrm{a},k} + \mathbf{n}_{\mathrm{a},k}, \boldsymbol{\omega}_k = \bar{\boldsymbol{\omega}}_k + \bar{\mathbf{b}}_{\mathrm{g},k} + \mathbf{n}_{\mathrm{g},k}, \tag{1}$$

where $\bar{\mathbf{a}}_k$ and $\bar{\boldsymbol{\omega}}_k$ are the true accelerations and angular velocities that are not measurable, $\bar{\mathbf{b}}_{\mathrm{a},k}$ and $\bar{\mathbf{b}}_{\mathrm{g},k}$ are unknown accelerometer and gyroscope time-varying stochastic biases, and $\mathbf{n}_{\mathrm{a},k}$ and $\mathbf{n}_{\mathrm{g},k}$ are accelerometer and gyroscope white noise components, modeled as zero-mean Gaussian with standard deviations of $\sigma_{\mathrm{a,N},k}$ and $\sigma_{\mathrm{g,N},k}$, respectively.

B. Alignment of Multiple Inertial Sensors

This paper denotes $\mathbf{u}_k^{ii}$ as a measurement vector collected by the ith calibrated IMU at time k and expressed in the sensor's own body frame. $\mathbf{u}_k^{ii} = \left[\mathbf{a}_k^{ii}, \boldsymbol{\omega}_k^{ii}\right]^\top$, where $\mathbf{a}_k^{ii}$ and $\boldsymbol{\omega}_k^{ii}$ represent accelerometer and gyroscope readings along the three axes, respectively. The acceleration and angular velocity measured by the ith IMU can also be expressed in the body frame of the jth IMU, denoted as $\mathbf{u}_k^{ij} = \left[\mathbf{a}_k^{ij}, \boldsymbol{\omega}_k^{ij}\right]^\top$.

Angular rates of $\boldsymbol{\omega}_k^{ii}$ and $\boldsymbol{\omega}_k^{ij}$ have the following relationships:

$$\boldsymbol{\omega}_k^{ij} = \mathbf{T}_i^j \boldsymbol{\omega}_k^{ii}, \tag{2}$$

where $\mathbf{T}_i^j$ is a Direct Cosine Matrix (DCM) transforming the body frame of ith IMU to the body frame of the jth IMU. Acceleration of $\mathbf{a}_k^{ii}$ and $\mathbf{a}_k^{ij}$ have the following relationships:

$$\mathbf{a}_k^{ij} = \mathbf{T}_i^j \mathbf{a}_k^{ii} + [\boldsymbol{\omega}_k^{ij}]_\times([\boldsymbol{\omega}_k^{ij}]_\times \mathbf{r}_i^j) + [\dot{\boldsymbol{\omega}}_k^{ij}]_\times \mathbf{r}_i^j. \tag{3}$$

In (3), $\dot{\boldsymbol{\omega}}_k^{ij}$ is angular acceleration, $[\mathbf{x}]_\times$ represents the skew-symetric matrix of a vector $\mathbf{x}$, and $\mathbf{r}_i^j$ represents the position of the ith IMU in the body frame of the jth IMU. The terms $[\boldsymbol{\omega}_k^{ij}]_\times([\boldsymbol{\omega}_k^{ij}]_\times \mathbf{r}_i^j)$ and $[\dot{\boldsymbol{\omega}}_k^{ij}]_\times \mathbf{r}_i^j$ in (3) correspond to the centrifugal force and the Euler force, respectively.

The DCM $\mathbf{T}_i^j$ and the position vector $\mathbf{r}_i^j$ in (2) and (3) are unknown and assumed to be time-independent values. In this paper, we followed the estimation algorithm discussed in [11] to determine the relative geometry $\mathbf{T}_i^j$ and $\mathbf{r}_i^j$ between two IMUs. Additionally, the angular acceleration $\dot{\boldsymbol{\omega}}_k^{ij}$ is calculated by taking the difference between two consecutive gyroscope measurements. That is, $\dot{\boldsymbol{\omega}}_k^{ij} = (\boldsymbol{\omega}_k^{ij} - \boldsymbol{\omega}_{k-1}^{ij})/\mathrm{dt}$, where dt is the sampling rate of the IMU. In this paper, we aligned all IMUs to the body frame of the 1st IMU, which has the best noise performance and lowest FSR and bandwidth.

C. Prioritization Mechanism

At time k, the proposed Prio-IMU chooses the accelerometer measurements collected by the IMU with the best noise performance among the IMUs that do not have saturated accelerometer measurements. The accelerometer white noise component $\mathbf{n}_{\mathrm{a},k}$ in (1) follows the noise characteristics of the chosen IMU. The choice mechanism can be mathematically expressed as follows:

$$\mathbf{a}_k = \mathbf{a}_k^{n1}, \sigma_{\mathrm{a,N},k} = \sigma_{\mathrm{a,N}}^{n}, \tag{4}$$

where

$$n = \min\{j \mid \forall 1 \leq i < j \leq N, |\mathbf{a}_k^{i1}| \geq \mathrm{F}_{\mathrm{a}}^{i} \text{ and } |\mathbf{a}_k^{i1}| < \mathrm{F}_{\mathrm{a}}^{i}\}.$$

With the nth IMU being chosen, this paper also estimates the time-varying accelerometer biases $\bar{\mathbf{b}}_{\mathrm{a},k}$ in (1). The estimated bias, denoted as $\mathbf{b}_{\mathrm{a},k}$, is updated at each time step as

$$\mathbf{b}_{\mathrm{a},k} = \mathbf{b}_{\mathrm{a},k}^{n1}, \tag{5}$$

where $\mathbf{b}_{\mathrm{a},k}^{ij}$ represents the estimated accelerometer stochastic time-varying bias of the ith IMU expressed in the body frame of the jth IMU. In our Prio-IMU, the stochastic biases $\mathbf{b}_{\mathrm{a},k}^{ij}$ of the accelerometer of the ith IMU are estimated based on unsaturated accelerometer measurements collected by the IMU with the best noise performance. At each timestamp k, $\mathbf{b}_{\mathrm{a},k}^{ij}$ is estimated as follows:

$$\mathbf{b}_{\mathrm{a},k}^{ij} = \mathbf{a}_{k-1}^{ij} - (\mathbf{a}_{k-1}^{lj} - \mathbf{b}_{\mathrm{a},k-1}^{lj}), \tag{6}$$

where lth IMU is chosen such that

$$l = \min\{m \mid \forall 1 \leq m \leq i, |\mathbf{a}_{k-1}^{mm}| \leq \mathrm{F}_{\mathrm{a}}^{m}\}.$$

A result of (6) is that $\mathbf{b}_{\mathrm{a},k}^{11} = \mathbf{0}$. This result was intended as the 1st IMU of the Prio-IMU has the lowest bias instability, and the available information from the other IMUs does not allow a more accurate estimation of the bias than zero.

The gyroscope readings of the proposed Prio-IMU, $\boldsymbol{\omega}_k$, are obtained with similar procedures discussed in (4)-(6).

III. Experimental Validation

A. Experimental Setup

To demonstrate the proposed Prio-IMU, we developed a Prio-IMU prototype, shown in Fig. 2. The current implementation of the system integrates a Teensy 4.0 microcontroller with an ICM-20948 6-Degree of Freedom (DoF) IMU, an ICM-20649 6-DoF IMU, and a 3-DoF ADXL375 accelerometer. Serial Peripheral Interface (SPI) communication protocol was used to communicate with all three sensors, and the sampling rate of the system was programmed at 1800 [Hz]. We experimentally characterized the three sensors, and the characteristics and the Allan deviation plots of each sensor are shown in Fig. 2.

Fig. 3 presents profiles of accelerometer and gyroscope measurements collected by the Prio-IMU prototype during the

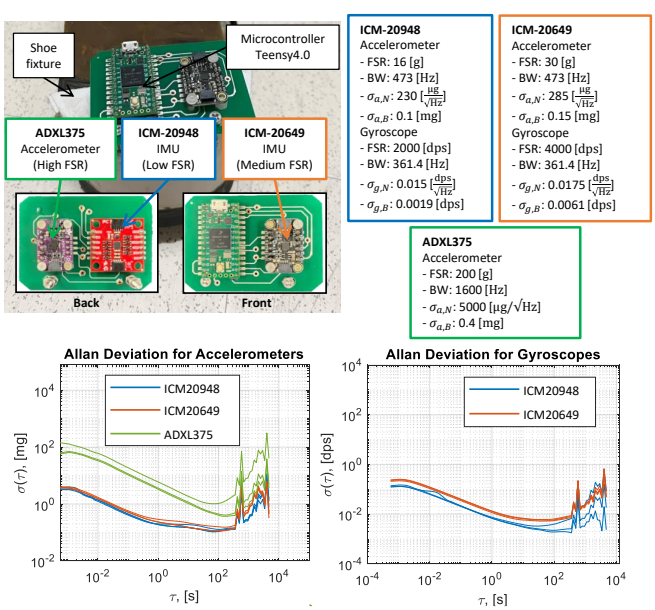

Fig. 2. A prototype of the proposed Prio-IMU and the characteristics of the deployed sensors.

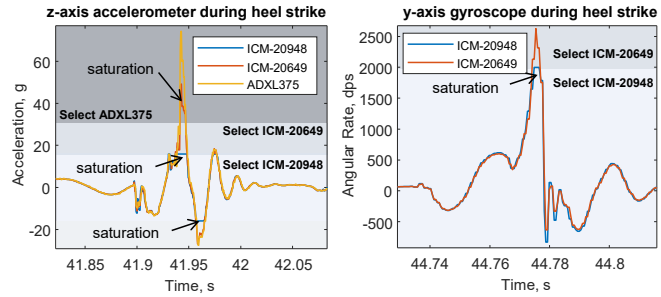

Fig. 3. Profiles of accelerometer and gyroscope measurements collected by the Prio-IMU prototype.

heel-strike phase of a running experiment. We could observe that the accelerometers of both ICM-20948 and ICM-20649 were saturated while the measurements of the ADXL375 were below the sensor accelerometer FSR of 200 [g]. It was also observed in Fig. 3 that the gyroscope measurements of the ICM-20948 were saturated at 2000 [dps] while the measurements of ICM-20649 peaked at around 2600 [dps].

B. Experimental Results

To validate the navigation performance of the proposed Prio-IMU, we conducted a series of 10 sets of pedestrian indoor navigation experiments at the University of California, Irvine. In each trial, a subject first walked a straight line for around 45 [m] at a pace of around 80 [steps per minute (spm)] and then ran a straight line for 42.8 [m] at a pace of around 180 [spm]. The total trajectory length was 87.8 [m]. We compared the navigation performance of the ZUPT-aided INS using four different configurations of the Prio-IMU prototypes. Each configuration used a unique combination of the three inertial sensors shown in Fig. 2. In this paper, we implemented the ZUPT-aided INS in an Extended Kalman Filter (EKF) framework with the Stance Hypothesis Optimal dEtection (SHOE) detector [3], [14]. Two fixed thresholds for the SHOE detector were determined, one for the case of walking and the other for running, such that the navigation errors were minimized.

Fig. 4 presents the experimental results using the four different configurations. We used the horizontal Root-Mean-Square-Errors (2D RMSEs), Circular Error Probables (CEPs), and vertical ($\perp$) RMSEs to evaluate each navigation solution. We could observe that Configuration 4, where all three sensors on the Prio-IMU prototype were used, had the minimum navigation errors, as compared to the other configurations. The experimental results proved that it is beneficial to use the proposed Prio-IMU to improve navigation accuracy in the case of foot-mounted IMUs.

Two remarks can be made on the developed Prio-IMU prototype. First, the quality of the Prio-IMU measurements was sensitive to errors in alignments of multiple IMUs. In our current approach, aligning the accelerometers of different IMUs, as discussed in (3), involved compensation of the centrifugal force and the Euler force, which required information of relative position vectors between each integrated IMU. The positions were results of algorithmic estimation with uncertainties. Moreover, the angular accelerations in

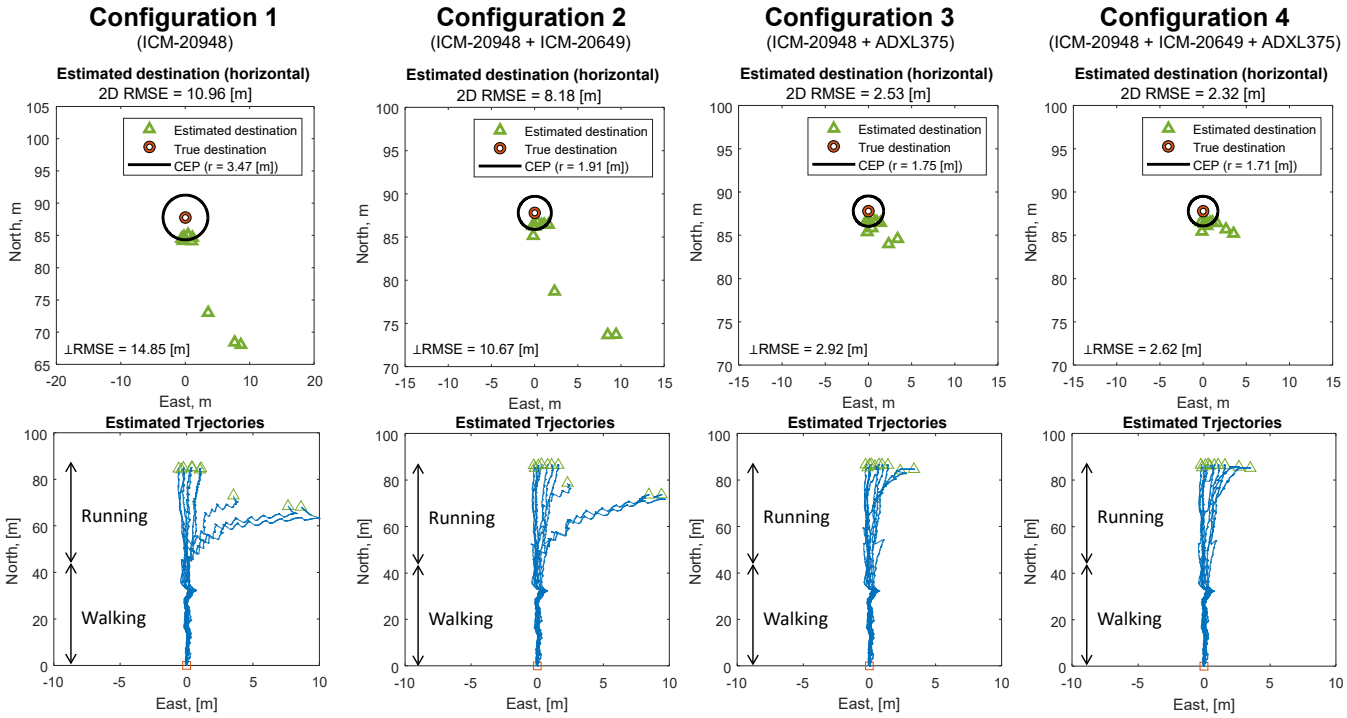

Fig. 4. Estimated trajectories of the experiments.

(3) were derived from gyroscope measurements by taking the derivative, which could introduce high-frequency noise components. One approach to reducing errors introduced by IMU alignment is to minimize displacements between each inertial sensor, and this could potentially be achieved through micro-fabrication technology. Second, the three inertial sensors integrated into the Prio-IMU prototype shown in Fig. 2 were chosen with a consideration of flexible development. The choice of sensors could be refined by not only increasing the FSR and bandwidth but also optimizing the noise performance of a particular axis of an accelerometer or gyroscope. For example, integrating an ultra-low-noise z-axis gyroscope could reduce the unobservable yaw angle errors in the ZUPT-aided INS, increasing the long-term navigation accuracy.

IV. Conclusion

This paper presents a Prio-IMU, a systematic approach utilizing multiple IMUs to simultaneously increase sensor FSR and bandwidth while maintaining great noise performance. We developed a Prio-IMU prototype integrating three different inertial sensors, and the experimental results involving walking and running showed that both the horizontal and vertical RMSEs of the ZUPT-aided INS using the Prio-IMU prototype were improved by 79% and 82%, as compared to the case of using a single ICM-20948 IMU. The approach showed a method for resolving trade-offs in selection of inertial sensors for foot-mounted IMUs in pedestrian navigation scenarios.

References

[1] R. Harle, "A survey of indoor inertial positioning systems for pedestrians," *IEEE Communications Surveys & Tutorials*, vol. 15, no. 3, pp. 1281–1293, 2013.

[2] E. Foxlin, "Pedestrian tracking with shoe-mounted inertial sensors," *IEEE Computer Graphics and Applications*, vol. 25, no. 6, pp. 38–46, 2005.

[3] C.-S. Jao, A. A. Abdallah, C. Chen, M.-W. Seo, S. S. Kia, Z. M. Kassas, and A. M. Shkel, "PINDOC: Pedestrian indoor navigation system integrating deterministic, opportunistic, and cooperative functionalities," *IEEE Sensors Journal*, vol. 22, no. 14, pp. 14424–14435, 2022.

[4] J. Wahlström and I. Skog, "Fifteen years of progress at zero velocity: A review," *IEEE Sensors Journal*, vol. 21, no. 2, pp. 1139–1151, 2020.

[5] E. Sangenis, C.-S. Jao, and A. M. Shkel, "SVM-based Motion Classification Using Foot-mounted IMU for ZUPT-aided INS," in *IEEE Sensors*, (Dalla, TX, USA), Oct 30-2, 2022.

[6] A. R. Parrish, C.-S. Jao, and A. M. Shkel, "Stance Phase Detection for ZUPT-Aided INS Using Knee-Mounted IMU in Crawling Scenarios," *IEEE Sensors Letters*, vol. 6, no. 5, pp. 1–4, 2022.

[7] Y. Wang and A. M. Shkel, "Adaptive threshold for zero-velocity detector in ZUPT-aided pedestrian inertial navigation," *IEEE Sensors Letters*, vol. 3, no. 11, pp. 1–4, 2019.

[8] C.-S. Jao and A. M. Shkel, "A reconstruction filter for saturated accelerometer signals due to insufficient FSR in foot-mounted inertial navigation system," *IEEE Sensors Journal*, vol. 22, no. 1, pp. 695–706, 2021.

[9] H. Ju, M. S. Lee, S. Y. Park, J. W. Song, and C. G. Park, "A pedestrian dead-reckoning system that considers the heel-strike and toe-off phases when using a foot-mounted IMU," *Measurement Science and Technology*, vol. 27, no. 1, p. 015702, 2015.

[10] H. Ju, J. H. Lee, and C. G. Park, "Pedestrian dead reckoning system using dual IMU to consider heel strike impact," in *18th International Conference on Control, Automation and Systems (ICCAS)*, (PyeongChang, GangWon Province, Korea), Oct 17-20, 2018.

[11] I. Skog, J.-O. Nilsson, P. Händel, and A. Nehorai, "Inertial sensor arrays, maximum likelihood, and cramér–rao bound," *IEEE Transactions on Signal Processing*, vol. 64, no. 16, pp. 4218–4227, 2016.

[12] H. Carlsson, I. Skog, and J. Jaldén, "Self-calibration of inertial sensor arrays," *IEEE Sensors Journal*, vol. 21, no. 6, pp. 8451–8463, 2021.

[13] Y. Wang, Y.-W. Lin, S. Askari, C.-S. Jao, and A. M. Shkel, "Compensation of systematic errors in zupt-aided pedestrian inertial navigation," in *IEEE/ION Position, Location and Navigation Symposium (PLANS)*, (Portland, Oregon, USA), April 20-23, 2020.

[14] I. Skog, P. Handel, J.-O. Nilsson, and J. Rantakokko, "Zero-velocity detection—An algorithm evaluation," *IEEE Transactions on Biomedical Engineering*, vol. 57, no. 11, pp. 2657–2666, 2010.